A novel closed-loop electromechanical stimulator to enhance osseointegration with immediate loading of dental implant restorations

J M Meswania[1,2]*, **V A Bousdras**[3], **S P Ahir**[1,2], **J L Cunningham**[4], **G W Blunn**[1,2], and **A E Goodship**[1,2,5]
[1]Institute of Orthopaedics and Musculoskeletal Science, University College London, London, UK
[2]Royal National Orthopaedic Hospital NHS Trust, London, UK
[3]UCL Eastman Dental Institute, London, UK
[4]Department of Mechanical Engineering, University of Bath, Bath, UK
[5]Royal Veterinary College, University of London, London, UK

The manuscript was received on 30 June 2009 and was accepted after revision for publication on 25 February 2010.

DOI: 10.1243/09544119JEIM686

Abstract: The degree of osseomechanical integration of dental implants is acutely sensitive to their mechanical environment. Bone, both as a tissue and structure, adapts its mass and architecture in response to loading conditions. Therefore, application of predefined controlled loads may be considered as a treatment option to promote early maturation of bone/implant interface prior to or in conjunction with crown/prosthesis attachment. Although many studies have established that the magnitude, rate of the applied strain, and frequency have significant effects on the osteogenic response, the actual specific relationships between strain parameters and frequency have not yet been fully defined. The purpose of this study was to develop a stimulator to apply defined mechanical stimuli to individual dental implants *in vivo* immediately after implantation, exploring the hypothesis that immediate controlled loading could enhance implant integration. An electromechanical device was developed, based on load values obtained using a two-dimensional finite element analysis of the bone/implant interface generating 1000 to 4000 με and operated at 30 and 3 Hz respectively. The device was then tested in a cadaveric pig mandible, and periosteal bone surface strains were recorded for potential future comparison with a three-dimensional finite element model to determine loading regimens to optimize interface strains and iterate the device for clinical use.

Keywords: dental implant, osseointegration, osteogenic stimuli, bone enhancement, biophysical forces

1 INTRODUCTION

Increasingly in dental practice, titanium implants are used to replace missing teeth in adults in a predictable manner with either a single implant crown or a multiunit system supporting a bridge or an overdenture. The advantage of this technique has been to provide a patient with masticatory function that is close to the natural teeth, giving the patient confidence and improved esteem.

*Corresponding author: UCL Institute of Orthopaedics and Musculoskeletal Science, University College London, RNOHT, Brockley Hill, Stanmore, Middlesex HA7 4LP, UK.
email: j.meswania@ucl.ac.uk*

The conventional practice is to use a protocol defined by Branemark *et al.* [**1**], which necessitates a two-stage process. First, the implants are inserted into the jawbone and are covered by the mucosa, followed by a minimum 3 to 6 month period to allow for osseointegration and maturation of the bone/implant interface by avoiding application of masticatory loads. After this period, the superstructure is fabricated in the form of a crown, a bridge, or an overdenture, and attached to the implant to complete the treatment. This delays functional loading and use of the implant for a period of months. Recently, one-stage treatment protocols, the effectiveness of which are reported by Engquist *et al.* [**2**] and Collaert and De Bruyn [**3**], have been developed

for patients using unsubmerged dental implants interconnected with superstructure to allow both immediate restoration and functional loading. However, the long-term outcome of this process is still unpredictable as this treatment modality was achieved 'empirically' with no scientific evidence related to the timing, magnitude, direction, and frequency of the applied masticatory loads, and the influence of these mechanical inputs on the bone quality and its properties. Therefore, a rationale is required to optimize integration through mechanobiology and avoid both early and long-term loosening.

Biological fixation of the dental implant relies greatly upon the bone quality, the surgical precision and induction of new bone formation that integrates with the macro, micro, and nano surfaces of the implant [**4**, **5**], and identification of the need to improve bony integration, particularly in patients with poor bone quality, such as the elderly in general and those with osteoporosis in particular. Alveolar crest bone loss surrounding the implant neck is a particularly common clinical phenomenon. This site-specific bone loss has been attributed to: (1) excessive load over a certain threshold and/or an inclined load producing lateral force [**6**, **7**] and (2) poor oral hygiene and alveolar bone density/properties [**8**]. In contrast, some researchers in the orthopaedic field have shown that artificially induced cyclic loads on implants and in the bone tissue itself can generate osteogenic strains that induce bone formation and bone regeneration, thus improving implant fixation and skeletal functional competence. Rubin and McLeod in 1994 [**9**] used a load cycle applied at 20 Hz producing $< 200\,\mu\varepsilon$ in sheep bone and achieved bony in-growth. Subsequently, Rubin *et al.* [**10**] and Oxlund *et al.* [**11**] both showed that even at $< 10\,\mu\varepsilon$ but at higher applied loading frequencies of 30–50 Hz, anabolic effects were generated in both cortical and trabecular bones. To see the effects at higher loads, Hollister *et al.* [**12**] induced $1000\,\mu\varepsilon$ at 3 Hz and observed new bone formation. Thus, dynamic loading with defined strain magnitudes applied at specific frequencies increases bone mass by stimulating osteogenic activity [**13**, **14**]. In essence, it is clear that the cyclic loading does produce an osteogenic response and that the range of stimulation frequency between 3 and 50 Hz osteogenic at low strain magnitudes is hypothesized as best suited for implant integration.

There is consensus among researchers that at a low stimulation frequency high strains are needed but at a high frequency low strains are appropriate to generate new bone. However, there is no systematic study so far to define exact relationships between applied strain magnitudes and loading frequency for osteogenic responses. Various researchers have evaluated specific environmental conditions such as reported by Carter *et al.* [**15**] and Smith-Adaline *et al.* [**16**]. Carter *et al.* have compared strain levels predicted by finite element (FE) analyses, with induction of connective tissue differentiation observed in developmental ossification and in fracture healing, while Smith-Adaline *et al.*, using a simplified fracture model of a rat bone exposed to a regular cyclic bending load, showed how bone formation occurs based on tensile or compressive elements of the strain field. Both of these findings suggest that the type of mechanical stimuli, i.e. compressive or tensile, greatly affects the way in which the bone regenerates. Smith-Adaline *et al.* suggest that under bending loading applied at 0.5 Hz during the fracture repair process, the intermittent tensile strains stimulated more cartilage formation in the short term, which then progressed to bone through endochondral ossification. The compressive strains produced considerably less cartilage but only gave a reduction in new bone formation of 20 per cent compared with the tensile loading. It is also important to understand that the microscopic strains at the cellular level can be extremely high compared to strains applied to the bulk of the material at the macroscopic level [**17**].

In contrast to orthopaedics, there is very limited information in the dental literature on mechanical stimulation of bone in the jaw and of dental implants. Biophysical forces, particularly mechanical loading and electromagnetic signals, are important regulators of bone formation and they have been applied successfully in craniofacial surgery [**18**]. Recently, Ko *et al.* [**19**] developed a customized intraoral hydraulic device to produce compressive force on the implant with a closed-loop control system, which avoided repeated anaesthesia by approaching the porcine oral cavity through a subcutaneous surgical approach. However, the subcutaneous approach can be considered as invasive and would not translate to clinical practice. Moreover, the study by Ko *et al.* [**20**] did not evaluate the strain surrounding freestanding implants; instead, they evaluated strains around splinted implants, as pin fixators were used medially and distally to the implant, offering apparatus stability by reducing micromotion.

Although the level of applied strain in the adjacent bone is the most important factor in creating osseointegration with an implant, it cannot be

measured directly nor controlled independently. In practice, an application of a load on the implant results in a range of tensile and compressive strains in the adjoining bone, with varying degrees of site-specific intensity. The strain profile within bone adjacent to an implant depends largely on the magnitude and direction of the applied load, the implant design, the extent of bone/implant contact, the proportion of cortical to cancellous bone in contact, the volume/geometry of each type of bone, and the bone 'quality'. However, it is important to impose and maintain the strain levels within the osteogenic range throughout the bone without causing such a high strain that would lead to bone resorption in localized areas while still engendering an osteogenic signal. Since the extent of bone contact and hence the magnitude of strain in any part of the bone cannot be determined consistently for every case, this might be an indication to choose high-frequency stimulation with a small load amplitude that cannot overstrain bone and cause resorption at the microscopic level. In addition to this, to help determine the degree of implant stability in clinical practice, a non-invasive technique such as the one described by Lachmann *et al.* [**21**] could be adopted to ascertain the appropriateness of a stimulation load.

There are a number of different actuator types that could be used to produce a direct mechanical load capable of inducing osteogenic strains on the implant. While pneumatic actuators can be compact [**22**], they are only suitable for low-frequency application (< 10 Hz) and can produce non-linear loads due to the compressibility of the working gas [**12**]. Piezoelectric devices can operate in a linear mode at almost any frequency, but the displacement produced is usually at the submicrometre level. Pulsed electromagnetic fields (PEMF) can provide a biophysical stimulus to bone cells in a non-invasive way. However, in a previous study [**23**], such PEMF stimulation (pulse width 85 μs, frequency 20 Mc, 30 min/day, 21 days) did not improve the bone integration process around dental implants placed in the rabbit tibia. Physical loads can also be applied by mechanical systems like vibrating motors [**11**], producing a 360° planar vector force per cycle, which might be too complex to quantify the bone response accurately.

The purpose of this developmental study was to design a mechanical stimulator using an electromagnetic linear motor that could apply compressive loads both at low (3 Hz) and at high (30 Hz) frequencies, while maintaining osteogenic strains around a single implant restoration, using a commercially available implant.

2 MATERIALS AND METHOD

2.1 Load determination

It is clear from the literature review that no prior publications for load determination exist that could be used for the development of this device, and therefore it was necessary to define a suitable load magnitude on a dental implant that creates a given range of strain level in the adjoining bone. As a preliminary indicator, the finite element (FE) method was used to analyse a two-dimensional surface-to-surface contact geometry of a commercially available dental implant placed in a simplified mandible geometry. Having developed a prototype device that is functionally acceptable, it could then be correlated against a future three-dimensional dynamic FE analysis to give a more accurate preclinical validation, which was outside the scope of this project.

A design of a cylindrical 11 mm microthread 4.0ST titanium implant (Astra Tech AB, Mölndal, Sweden) with a 4 mm outside diameter and a threaded external surface (Fig. 1) was used for the FE analysis. The moduli used were linear and elastic, and given the values for stiffness of 110 GPa for the implant (obtained from material specifications), 15 GPa for the cortical bone [**24**], and 0.3 GPa for the cancellous bone. A Poisson ratio of 0.3 was used for each material. The thickness of cortical bone was assumed to be 2 mm at the crest of the mandibular ridge, and the remaining implant was in full contact with cancellous bone. The analysis was performed in MARC 2003 (MSc Software, USA), where the implant

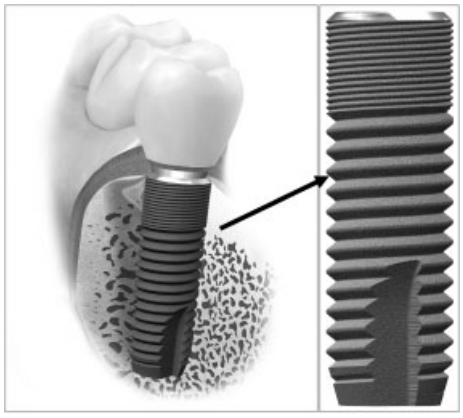

Fig. 1 A typical 4.0ST titanium dental implant (from marketing literature, Courtesy of Astra Tech AB)

was able to move relative to the bone, performing a contact analysis with no friction, as expected initially after implantation.

The lower end of the two-dimensional section of the bone was held rigidly to prevent free body motion, and a static load was applied to the implant (Fig. 2(a)), which varied from 5 to 30 N. The mesh consisted of two-dimensional planar four-node quadrilateral elements. For the implant 70 278 elements and 72 188 nodes were used, and for the bone 32 669 elements and 34 980 nodes. The mesh density was varied with finer meshes at the bone/implant interface, as shown in the inset in Fig. 2(a), to improve accuracy. The bone was defined with two material properties representing cortical and cancellous regions. The contact analysis was defined as consisting of two bodies: implant and bone. The analysis performed on the structure was static and linear with contact analysis. The maximum and minimum principal strains were then determined. An example of the strain distribution obtained is shown in Fig. 2(b). The maximum principal strains occurred at the base of the thread interface of the bone. Since the amount of bone formation inside the thread ridges is important for implant stability and longevity, prevention of bone resorption in this region is important, and therefore maximum principal strain values at two elements from the interface were examined and are plotted in Fig. 2(c).

2.2 Calliper design

Having established the approximate load level, a prototype device was constructed. A schematic is shown in Fig. 3 and a photograph of the calliper being used in a cadaveric Berkshire pig mouth is shown in Fig. 4. The device consisted of a pair of calliper arms, a linear motor, a displacement transducer, and a hard acrylic splint. At one end of the calliper, the motor body was connected to the lower arm with the plunger connected to the motor pushing the upper arm. At the other end of the calliper, a splint was positioned intraorally over the mandibular premolars distal to the implant that was to be stimulated, and a base plate was stabilized over the occlusal surfaces of the maxillary premolars with the link held tightly between them, thus creating a stable strut arrangement across the upper and lower jaws. In clinical practice, the device is designed to be held in place by closing the mouth and holding it tight by the jaw muscles, but in this cadaveric trial, the mouth-closing force was applied with hands tightly holding them together. Attached to the splint was the other end of the lower arm, thus creating a rigid fixation to carry the reaction force from the anvil. While the lower arm was held rigidly in place, the anvil attached to the upper arm loaded the implant.

This mechanical arrangement provided easy positioning of the anvil over the implant. The force produced on the implant was measured by strain gauges mounted on the upper arm. The position of the pivot point was such that the force generated by the linear motor was amplified mechanically by a factor of 2:1. A three-phase inverter drove the linear motor where the feedback from a displacement transducer incorporated within the motor produced a controlled force displacement in response to an applied sinusoidal reference signal set at 0–10 V peak-to-peak. The linear motor and the control electronics were supplied by Copley Controls Corporation, USA.

2.3 Load validation

To validate the data logging software, the input sine wave signal was sampled directly for a period of 10 s at both 3 and 30 Hz frequencies. The equipment was then attached to a 1 kN calibration load cell (Kistler Instruments) where the lower jaw was clamped in a vice, as it would be held in the mouth, with the upper arm pushing on to the implant represented by the load cell (Fig. 5). Two sets of readings were obtained from stimulator and load cell outputs at both frequencies. Sampling rates for both data logging systems were 1200 Hz (40 times the highest frequency being measured, well above the 10 times suggested by the Nyquist sampling theorem to gain good resolution), and the output resolutions were matched as close as practical.

2.4 Operational verification

To validate the prototype device for practicality, a cadaveric Berkshire pig head implanted with two 11 mm Astra Tech implants (4.0ST cylindrical), one on the left first premolar site and one in the same position on the opposite side, was prepared (Fig. 6). Surgical and restorative protocols are described elsewhere [**25**]. Following soft tissue removal and bone drying using alcohol, two 45° foil strain gauge rosettes (350 Ω with a gauge factor of 2.15 – Tokyo Sokki Kenkyujo Co. Ltd) were applied using cyanoacrylate adhesive on both lingual and buccal cortices. The middle gauge of each rosette was oriented in the direction parallel to the implant axis. The

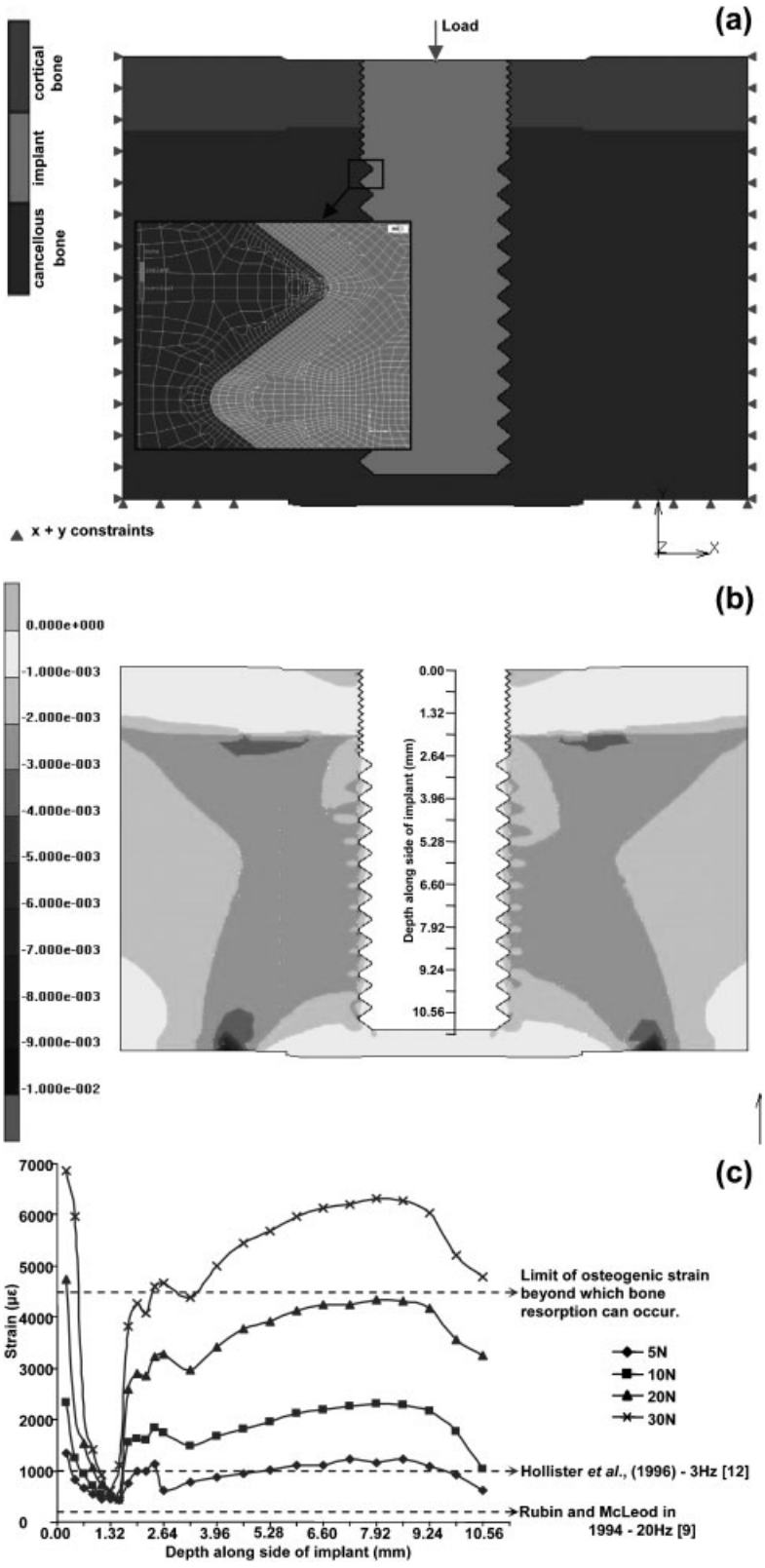

Fig. 2 A 2D finite element analysis model with a 2 mm cortical bone layer at the top and cancellous bone underneath: (a) model geometry with constraints and elements; (b) a typical strain distribution within the bone with a 10 N implant load (implant not shown); (c) maximum strain recorded in the bone within each thread profile at 2 elements (distance ~ 0.03 mm) from the implant–bone interface produced by 5, 10, 20, and 30 N implant loads

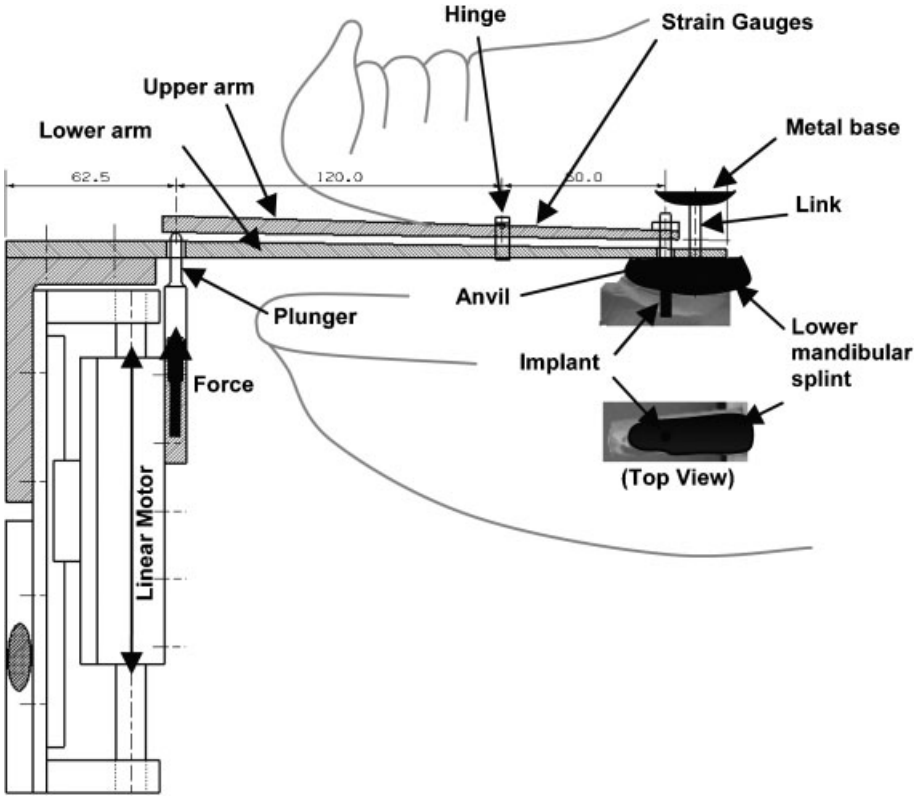

Fig. 3 Schematic of the mechanical system and intraoral position of the calliper and splint/anvil assembly in a cadaveric pig mouth

implant in the left first premolar side was randomly selected for mechanical stimulation at 3 and 30 Hz, while the implant in the right first premolar side served as a control. Principal strains were subsequently calculated for each rosette site using the two-dimensional elastic strain relationship.

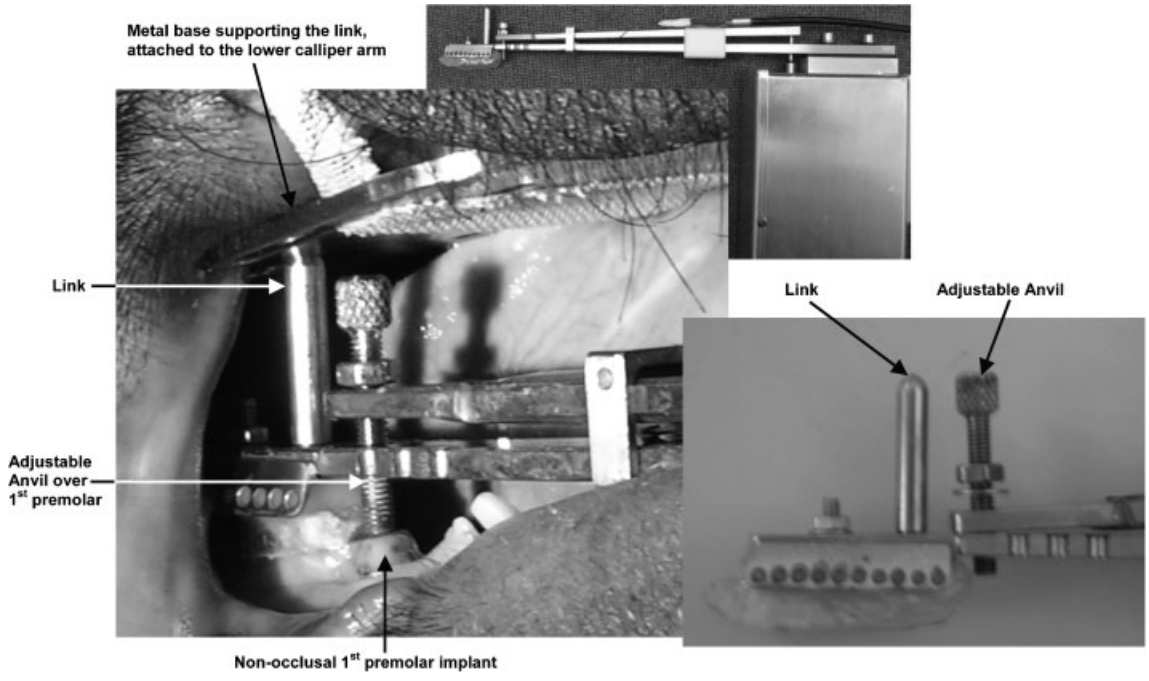

Fig. 4 The actual prototype device and intraoral position of the calliper and splint/anvil assembly in a cadaveric pig mouth

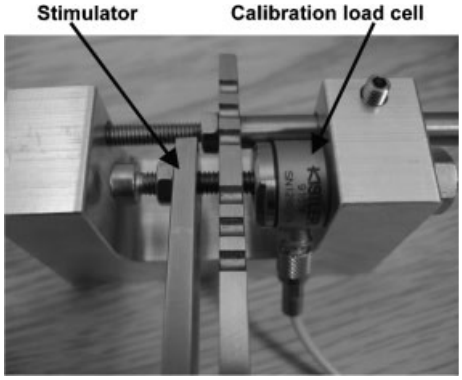

Fig. 5 Stimulator mounted against a calibration load cell

3 RESULTS

3.1 Load determination

The two-dimensional finite element analysis showed that for a 4.0ST titanium implant with a 4 mm diameter and a threaded external surface, the stimulation device needed to produce 5 N to induce 1000 με and 20 N to induce 4000 με in the surrounding bone (see Fig. 2(c)). In addition, to ensure that the bone was not overstrained, the peak load was restricted to a maximum of 25 N. Thus, to examine the stimulator characteristics, the frequencies chosen were 3 Hz, producing a 20 N load on the implant giving low-frequency high-load stimulation for one extreme, and 30 Hz producing 5 N giving high-frequency low-load stimulation for the other extreme.

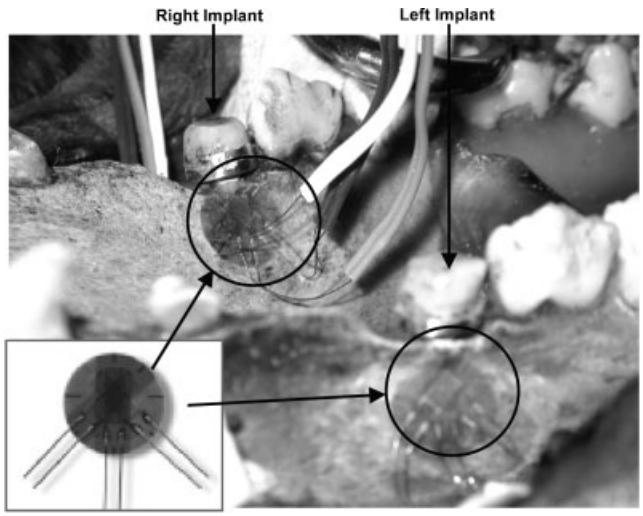

Fig. 6 Two implants in both left and right first premolar positions with crowns attached in a cadaveric pig mandible with strain gauge rosettes attached to both lingual and buccal cortices

3.2 Load validation

Output from a signal generator at 3 and 30 Hz was recorded and evaluated using fast Fourier transformation (FFT) analysis to ensure purity of the signal. Signals obtained are shown in Fig. 7(a), where, for clarity, only half a second sampling period is shown. The FFT analysis verified primary frequencies in both cases to be a perfect match, as shown in Figs 7(b) and (c) respectively. However, for both frequencies there were secondary peaks at three times the stimulation frequencies that are just about visible on both graphs. These secondary peaks,

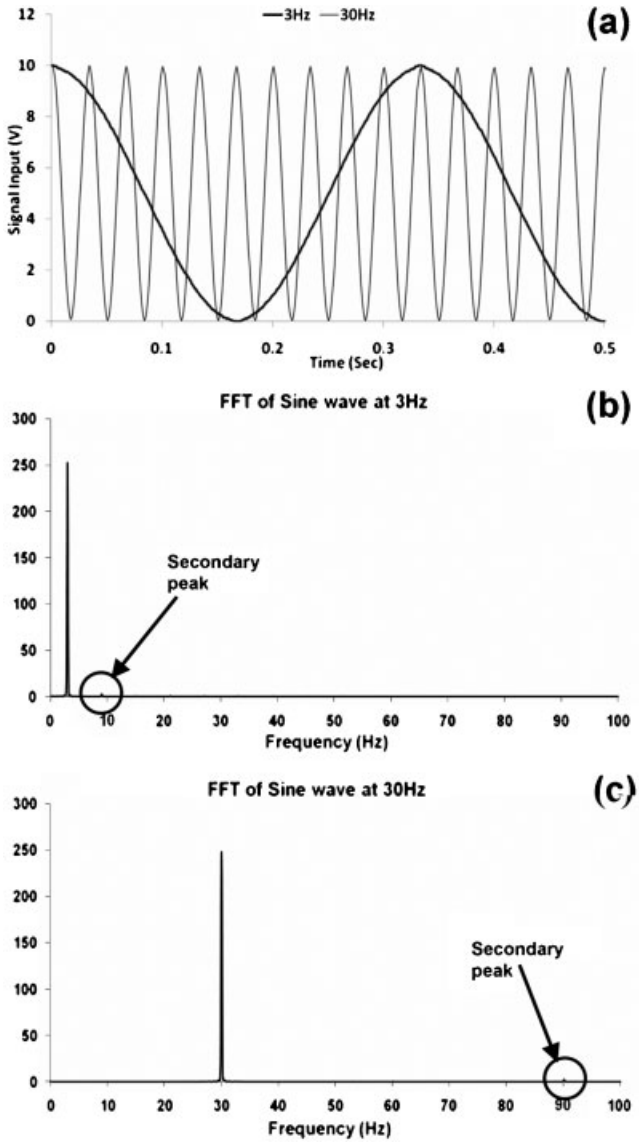

Fig. 7 Signal generator: (a) input signals at 3 and 30 Hz; (b) fast Fourier transformation (FFT) analysis for the 3 Hz signal; (c) FFT analysis for the 30 Hz signal. Both analyses show one insignificant secondary peak

which were thought to have been caused by the sampling rate (quantization), were extremely small in comparison with the primary frequencies and were hence considered negligible.

Outputs from a calibration load cell attached to the stimulator at 3 and 30 Hz stimulation frequencies are shown in Fig. 8(a), with corresponding FFT results in Figs 8(b) and (c) respectively. The graphs show that although the primary frequencies were exact in both cases, the load profile at 3 Hz was skewed, while at 30 Hz it matched well with the input signal. FFT analysis for 30 Hz data showed that there was a very small secondary peak at three times the stimulation frequency, just as in the input signal shown in Figs 7(c), and there were no other harmonics for this loading condition. This, as before, was thought to be the result of the sampling rate (quantization) and, being extremely small in comparison with the primary frequency, it was considered negligible. For 3 Hz, however, there were harmonics at approximately 6 Hz increments, with the last peak occurring at about 22 Hz, the highest peak being 10.8 per cent of the primary frequency occurring at about 15 Hz. The fact that harmonics were observed against a load cell indicated this to be a characteristic property of the stimulator itself. Possible sources for the harmonics could be the mechanical arms being operated close to the natural frequency or the motor lacking in capacity; this needs further investigation. The same result showed that a constant 0–10 V peak-to-peak input signal resulted in a 22 N peak-to-peak load at 3 Hz, and a 6 N peak-to-peak load at 30 Hz.

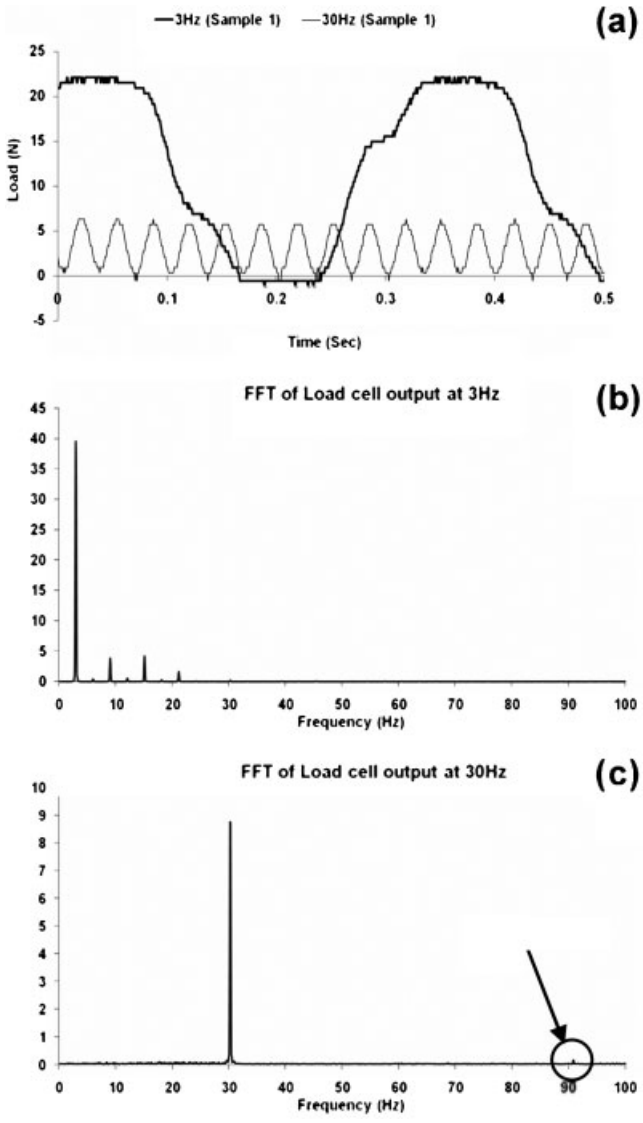

Fig. 8 Calibration load cell output: (a) load measured at the point of application for 3 and 30 Hz; (b) fast Fourier transformation (FFT) analysis for 3 Hz showing three significant secondary peaks; (c) FFT analysis for 30 Hz showing one insignificant secondary peak

The output from the strain gauges mounted on the stimulator arm and monitored using a custom-built data logging system at 3 and 30 Hz is shown in Fig. 9. Unfortunately, the custom-built data logging system used for this measurement had an inherent error, causing data starvation, as indicated by the vertical arrows. For this reason, the load data measured from these strain gauges were not validated, as the equipment was destined for modification. However, the amplitude of applied load indicated by the strain gauge output compared well with the amplitude measured by the load cell (Fig. 8(a)) at both stimulation frequencies, indicating a good correlation of the measured strain as an indicator of load.

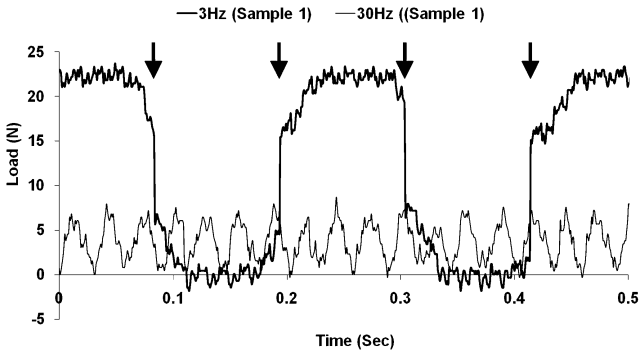

Fig. 9 Output from the strain gauges mounted on the stimulator. The vertical lines (marked with arrows) for the 3 Hz signal show clearly the regular occurrence of data starvation. Note that there should only be 1.5 cycles for a half a second period. Load applied on the implant is as indicated by the amplitude at both frequencies

3.3 Operational verification

The device was used to measure strains on the cortical bone surfaces adjacent to implants mounted in a cadaveric pig mandible at both left and right first premolar sites. Principal strains adjacent to the stimulated implant for both loading frequencies are shown in Figs 10(a) and (b). Likewise, principal strains adjacent to the non-stimulated implant mounted as a control on the opposite side of the mouth are shown in Figs 10(c) and (d). These strains were recorded for 10 s, which included initial settling-in, and therefore only the last one second is shown here. The strain oscillation in response to the applied stimulation load was clearly identifiable for the loaded implant side and was also in evidence on the control side. This was probably due to the elastic nature of the whole mouth, where the load applied to one side of the mouth influenced the bone strain on the other side. However, more importantly, what the graphs also show is that there was a static strain built into the jawbone by virtue of holding the jaws tightly closed over the link in order to provide a stable fixation for the stimulator. This, in a living person, would be applied through the jaw muscles closing the mouth over the device and holding it tight. Therefore, with this technique of implant stimulation, there will always be a static strain field present, which would then be augmented by the stimulation force. The oscillating stimulation force also generated a vibration throughout the whole bone structure. The maximum principal strains created by cyclic loading at the gauge site were 29 με at 3 Hz and 14 με at 30 Hz on the buccal side and 27 με at 3 Hz and 7 με at 30 Hz on the lingual side.

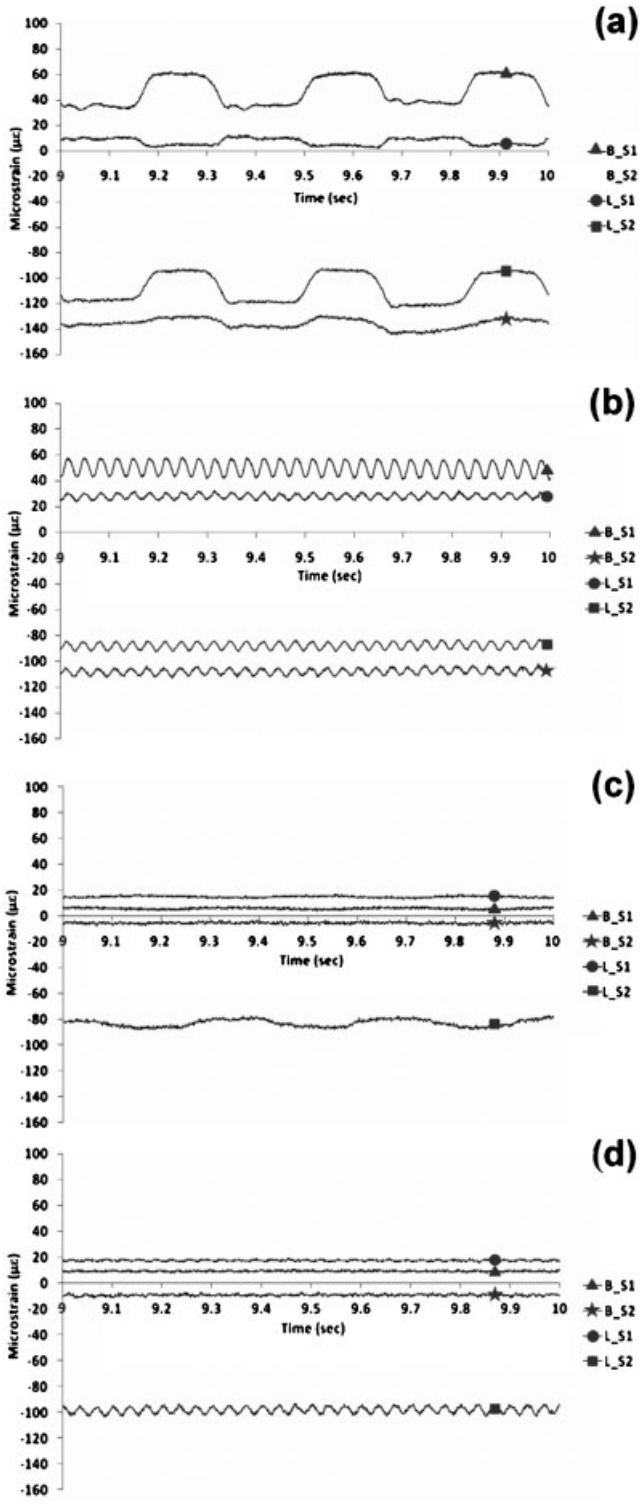

Fig. 10 Cortical surface strains in a cadaveric pig mandible: (a) 3 Hz stimulated implant; (b) 30 Hz stimulated implant; (c) 3 Hz control implant; (d) 30 Hz control implant (where B = buccal, L = lingual, and S1 and S2 are two principal strains at the gauge sites)

4 DISCUSSION

This electromechanical device provides one possible way of inducing controlled low-energy cyclic loads in a dental implant to induce osteogenic strains at the bone/implant interface. Since this stimulator was constructed solely based on the results from a two-dimensional FE analysis, further analytical work is recommended. The models used in this paper cannot be quantitatively validated by a clinical study, but such simplifications are considered reasonable for a comparative initial study. Due to the complexity of the implant/jawbone systems, a variety of factors may influence the mechanical fields in either bone or implants.

In the present study, several assumptions were made for the finite element analysis. The two bone

materials, cortical and cancellous, were assumed to be linearly elastic, whereas a non-linear assumption may be more appropriate for the simulation of the jawbone. In addition, the shape of the geometry was simplified. A more realistic three-dimensional analysis with specific architecture may provide more accurate information on stress/strain fields, thus ascertaining that the applied load does in fact match osteogenic bone strain adjacent to the implant, particularly where the cancellous cavity is asymmetric, which could cause a large variation in the circumferential load transfer. A computer tomography (CT) scan of the cadaver model used in this study could be used to generate FE analysis where more realistic shape and boundary conditions could be applied and compared with the cortical surface strains measured using strain gauges. The current model does not allow this comparison to be made.

A previous FE study reported by Qian *et al.* [**26**] similarly used a simplified three-dimensional mandible to assess the effect of applied load from different angles, but the study assumed full bonding at the bone/implant interface representing full integration. Another study by Guan *et al.* [**27**] used an interface condition with 50 per cent bonding over the entire contact surface by allowing pockets of blood deep within a thread form of the implant. The limitations of both of these studies are that they do not represent the contact interface and the loads specific for the immediate post-implantation condition. The present study, although a two-dimensional analysis, was performed using contact analysis between the implant and bone with no friction. Recently, mathematical models have been developed [**28**, **29**] to predict bone resorption over time, providing further insight into the bone regeneration process; currently these findings are compared to clinical observations.

Dynamic loading in the FE analysis could be investigated to provide more realistic data regarding strain levels in the bone, which could provide enhanced validation against actual clinical use. The information gained from dynamic FE analysis could further help to understand the role of frequency levels, resonance characteristic of the jawbone, bone formation, and the way in which strain level is influenced by these factors. The relationship between frequency level and bone formation has been investigated by a number of investigators [**30**–**32**], but to date there has not been any published categorized information. There may well be an optimum relationship between strain rate and the rate of remodelling response at different load levels. Ascertaining this information is important but was considered to be outside the scope of the present study. However, investigation of these parameters could be the subject of future work.

In terms of the functionality of the device, it clearly demonstrated against a load cell where the applied frequency was in fact in unison with the input frequency and that the harmonic interference was negligible for 30 Hz. However, the harmonics were significant for the 3 Hz stimulation, where the secondary peak occurred at about 15 Hz. This was due to the calliper arms being relatively flexible, producing a large deflection at higher loads with which the motor control system was unable to keep pace. This delayed response by the motor is clearly seen in the graph shown in Fig. 8. It is also possible that, at 3 Hz, the mechanical components of the stimulator were being operated close to the natural frequency of these parts, which may have contributed to the way in which the motor responded; this needs further investigation. With the input signal set at 0–10 V peak-to-peak, increasing frequency from 3 to 30 Hz resulted in the implant load reducing from 22 to 6 N. This reduction in force at the higher frequency is caused by higher energy absorption by the moving parts of the motor. Therefore, it is recommended that a lighter-weight motor be used in combination with more rigid calliper arms that require less displacement, thus improving motor performance.

The relatively large linear motor attached to the calliper was comparatively heavy, difficult to handle, and required support during use. Since the moving parts of the motor required energy to overcome the inertial effects, the orientation of the motor was also very critical. A horizontally positioned motor produced a much better response than a vertically positioned one where the gravitational effects were significant. Instead of a linear motor, a rotary motor might provide better directional insensitivity, but this should be considered as an alternative with caution since the load vector produced in this instance would be axial as well as tangential in relation to the long axis of the implant. The calliper itself functioned well and customization of the splints to suit individual geometries was easy to achieve. The technique of applying an oscillating load axially on to an implant was demonstrated to be remarkably simple and this has provided a baseline for future developments. Any new generation must be portable and easy to use by the patients themselves in their own homes, since this treatment is expected to last for a number of weeks post-implantation and will need to be applied daily.

5 CONCLUSION

The electromechanical device proposed in this study has shown frequency and load reproducibility measured against a calibrated load cell. This has demonstrated the ability of the mechanical stimulator device to generate the required loading at the chosen two frequencies. Moreover, the verification test demonstrated harmonic frequency values of negligible significance at 30 Hz stimulation. Harmonic frequencies of higher values at 6 Hz increments were recorded for the 3 Hz stimulation at the point of load application. Theoretically, this might have an effect on the final applied loading regimen and its suggested osteogenic potential. If the production of osteogenic strain is the prime objective, then this can be taken as a positive characteristic of the device. Leaving these issues aside, which are considered easily rectifiable in the next iteration of this device, this electromagnetic linear motor system was considered appropriate for producing the required loads at 3 and 30 Hz frequencies and capable of inducing the osteogenic strains at the bone/implant interface.

ACKNOWLEDGEMENTS

This investigation was supported by an EC grant ('IMLOAD: improving implant fixation by immediate loading', QLK6-CT-2002-02442). In addition, the provision of confidential implant geometry characteristics by Dr Stig Hansson (Astra Tech AB, Mölndal, Sweden) is acknowledged. The authors declare no commercial association with the products cited herein.

REFERENCES

1 **Branemark, P. I., Zarb, G. A.,** and **Albrektsson, T.** *Tissue integrated prosthesis: osseointegration in clinical dentistry*, 1985, pp. 199–209 (Quintessence Publishing, Chicago, Illinois).

2 **Engquist, B., Astrand, P., Anzen, B., Dahlgren, S., Engquist, E., Feldmann, H., Karlsson, U., Nord, P. G., Sahlholm, S.,** and **Svardstrom, P.** Simplified methods of implant treatment in the edentulous lower jaw: a 3-year follow-up report of a controlled prospective study of one-stage versus two-stage surgery and early loading. *Clin. Implant Dent. Related Res.*, 2005, **7**, 95–104.

3 **Collaert, B.** and **De Bruyn, H.** Comparison of Branemark fixture integration and short-term survival using one-stage or two-stage surgery in completely and partially edentulous mandibles. *Clin. Oral Implants Res.*, 1998, **9**, 131–135.

4 **Ericsson, N. K.** Early functional loading using Branemark dental implants. *Int. J. Periodontics Restorative Dent.*, 2002, **22**, 9–19.

5 **Pelayo, J. L., Diago, Miguel P., Bowen, E. M.,** and **Diago, Maria P.** Intraoperative complications during oral implantology. *Med. Oral Patol. Oral Cir. Bucal.*, 2008, **13**, E239–E243.

6 **Isidor, F.** Loss of osseointegration caused by occlusal load of oral implants. A clinical and radiographic study in monkeys. *Clin. Oral Implants Res.*, 1996, **7**(2), 143–152.

7 **Duyck, J., Ronold, H. J., Van Oosterwyck, H., Naert, I., Vander Sloten, J.,** and **Ellingsen, J. E.** The influence of static and dynamic loading on marginal bone reactions around osseointegrated implants: an animal experimental study. *Clin. Oral Implants Res.*, 2001, **12**(3), 207–218.

8 **Heitz-Mayfield, L. J., Schmid, B., Weigel, C., Gerber, S., Bosshardt, D. D.,** and **Jonsson, J.** Does excessive occlusal load affect osseointegration? An experimental study in the dog. *Clin. Oral Implants Res.*, 2004, **15**(3), 259–268.

9 **Rubin, C. T.** and **McLeod, K. J.** Promotion of bony ingrowth by frequency-specific, low-amplitude mechanical strain. *Clin. Orthop. Related Res.*, 1994, **298**, 165–174.

10 **Rubin, C. T., Sommerfeldt, D. W., Judex, S.,** and **Qin, Y.** Inhibition of osteopenia by low magnitude, high-frequency mechanical stimuli. *Drug Discov. Today*, 2001, **6**(16), 848–858.

11 **Oxlund, B. S., Ortoft, G., Andreassen, T. T.,** and **Oxlund, H.** Low-intensity, high-frequency vibration appears to prevent the decrease in strength of the femur and tibia associated with ovariectomy of adult rats. *Bone*, 2003, **32**, 69–77.

12 **Hollister, S. J., Guldberg, R. E., Kuelske, C. L., Caldwell, N. J., Richards, M.,** and **Goldstein, S. A.** Relative effects of wound healing and mechanical stimulus on early bone response to porous-coated implants. *J. Orthop. Res.*, 1996, **14**(4), 654–662.

13 **Rubin, C. T.** and **Lanyon, L. E.** Regulation of bone formation by applied dynamic loads. *J. Bone Jt Surg. Am.*, 1984, **66**(3), 397–402.

14 **Hillam, R. A.** and **Skerry, T. M.** Inhibition of bone resorption and stimulation of formation by mechanical loading of the modelling rat ulna *in-vivo*. *J. Bone Miner. Res.*, 1995, **10**(5), 683–689.

15 **Carter, D. R., Beaupre, G. S., Giori, N. J.,** and **Helms, J. A.** Mechanobiology of skeletal regeneration. *Clin. Orthop. Related Res.*, 1998, S41–S55.

16 **Smith-Adaline, E. A., Volkman, S. K., Ignelzi Jr, M. A., Slade, J., Platte, S.,** and **Goldstein, S. A.** Mechanical environment alters tissue formation patterns during fracture repair. *J. Orthop. Res.*, 2004, **22**, 1079–1085.

17 **Nicolella, D. P., Bonewald, L. F., Moravits, D. E.,** and **Lankford, J.** Measurement of microstructural strain in cortical bone. *Eur. J. Morphol.*, 2005, **42**, 23–29.

18 **Meyer, U., Kruse-Losler, B.,** and **Wiesmann, H. P.** Principles of bone formation driven by biophysical forces in craniofacial surgery. *Br. J. Oral Maxillofac. Surg.*, 2006, **44**(4), 289–295.
19 **Ko, C. C., Swift, J. Q., Delong, R., Douglas, W. H., Kim, Y. I.,** and **An, K. N.** An intra-oral hydraulic system for controlled loading of dental implants. *J. Biomechanics*, 2002, **35**(6), 863–869.
20 **Ko, C. C., Douglas, W. H., Delong, R., Rohrer, M. D., Swift, J. Q.,** and **Hodges, J. S.** Effects of implant healing time on crestal bone loss of a controlled-load dental implant. *J. Dent. Res.*, 2003, **82**(8), 585–591.
21 **Lachmann, S., Jager, B., Axmann, D., Gomez-Roman, G., Groten, M.,** and **Weber, H.** Resonance frequency analysis and damping capacity assessment. Part I: an *in-vitro* study on measurement reliability and a method of comparison in the determination of primary dental implant stability. *Clin. Oral Implants Res.*, 2006, **17**, 75–79.
22 **Lipscomb, V. J., Lawes, T. J., Goodship, A. E.,** and **Muir, P.** Asymmetric densitometric and mechanical adaptation of the left fifth metacarpal bone in racing greyhounds. *Vet. Rec.*, 2001, **148**(10), 308–311.
23 **Buzza, E. P., Shibli, J. A., Barbeiro, R. H.,** and **Barbosa, J. R.** Effects of electromagnetic field on bone healing around commercially pure titanium surface: histologic and mechanical study in rabbits. *Implant Dent.*, 2003, **12**(2), 182–187.
24 **Choi, K., Kuhn, J. L., Ciarelli, M. J.,** and **Goldstein, S. A.** The elastic moduli of human subchondral, trabecular, and cortical bone tissue and the size-dependency of cortical bone modulus. *J. Biomechanics*, 1990, **23**(11), 1103–1113.
25 **Bousdras, V., Sindet-Pedersen, S., Cunningham, J. L., Blunn, G., Petrie, A., Naert, I. E., Jaecques, S.,** and **Goodship, A. E.** Immediate functional loading of single-tooth TiO_2 grit-blasted implant restorations: a controlled prospective study in a porcine model. Part I: clinical outcome. *Clin. Implant Dent. Related Res.*, 2007, **9**, 197–206.
26 **Qian, L., Todo, M., Matsushita, Y.,** and **Koyano, K.** Effects of implant diameter, insertion depth, and loading angle on stress/strain fields in implant/jawbone systems: finite element analysis. *Int. J. Oral Maxillofac. Implants*, 2009, **24**(5), 877–886.
27 **Guan, H., van Staden, R., Loo, Y., Johnson, N., Ivanovski, S.,** and **Meredith, N.** Influence of bone and dental implant parameters on stress distribution in the mandible: a finite element study. *Int. J. Oral Maxillofac. Implants*, 2009, **24**(5), 866–876.
28 **Li, J., Li, H., Shi, L., Fok, A. S., Ucer, C., Devlin, H., Horner, K.,** and **Silikas, N.** A mathematical model for simulating the bone remodeling process under mechanical stimulus. *Dent. Mater.*, 2007, **23**(9), 1073–1078.
29 **Chou, H. Y., Jagodnik, J. J.,** and **Müftü, S.** Predictions of bone remodeling around dental implant systems. *J. Biomechanics*, 2008, **41**(6), 1365–1373.
30 **O'Connor, J. A., Lanyon, L. E.,** and **MacFie, H.** The influence of strain rate on adaptive bone remodelling. *J. Biomechanics*, 1982, **15**(10), 767–781.
31 **Pérez, M. A., Moreo, P., García-Aznar, J. M.,** and **Doblaré, M.** Computational simulation of dental implant osseointegration through resonance frequency analysis. *J. Biomechanics*, 2008, **41**(2), 316–325.
32 **Pattijn, V., Van Lierde, C., Van der Perre, G., Naert, I.,** and **Vander Sloten, J.** The resonance frequencies and mode shapes of dental implants: rigid body behaviour versus bending behaviour. A numerical approach. *J. Biomechanics*, 2006, **39**(5), 939–947.

APPENDIX

Units

GPa	gigapascal
Hz	Hertz
mm	millimetre
N	Newton
s	second
V	volt
$\mu\varepsilon$	microstrain
Ω	ohm